Available online at www.sciencedirect.com
ScienceDirect
Journal of the European Ceramic Society 31 (2011) 2691–2698
www.elsevier.com/locate/jeurceramsoc

Processing of yttria stabilized zirconia reinforced with multi-walled carbon nanotubes with attractive mechanical properties

Mehdi Mazaheri [a,*], Daniele Mari [a], Robert Schaller [a], Guillaume Bonnefont [b], Gilbert Fantozzi [b]

[a] *Ecole Polytechnique Fédérale de Lausanne (EPFL), Laboratoire de Physique de la Matière Complexe (LPMC), CH-1015 Lausanne, Switzerland*
[b] *INSA-Lyon, MATEIS CNRS UMR 5510, 20 Av. Albert Einstein, F-69621 Villeurbanne Cedex, France*

Available online 9 December 2010

Abstract

The improvement of the mechanical properties of carbon nanotube reinforced polycrystalline yttria-stabilized zirconia (CNT–YSZ) was questionable in earlier investigations due to several difficulties for processing of these composites. In the present article, the authors are proposing a successful technique for mixing pre-dispersed CNTs within YSZ particles followed by a fast spark plasma sintering at relatively low temperature, resulting in near full-dense structure with well-distributed CNTs. Composites with CNT quantities ranging within 0.5–5 wt% have been analyzed and a significant improvement in mechanical properties, i.e. Young's modulus, indentation hardness and fracture toughness with respect to monolithic YSZ could be observed. To support these interesting mechanical properties, high-resolution electron microscopy and Raman spectroscopy measurements have been carried out. The analysis of densification shows that the lower densification rate of CNT reinforced composites with respect to the pure YSZ could be attributed to a slower grain boundary sliding or migration during sintering.

Keywords: Zirconia; Carbon nanotubes; Processing; Nanocomposite; Fracture toughness

1. Introduction

During the last decade, the extraordinary mechanical, electrical and thermal properties of carbon nanotubes (CNTs) have encouraged the researchers to process CNT contained composites in order to improve the host matrix properties.[1] While high strength, hardness and thermal–chemical stability of ceramics are promising for several applications, their brittleness prevents from their use in many applications. The incorporation of CNTs, in analogy to traditional ceramic composites reinforced with micrometric fibers, is often aimed at enhancing the fracture toughness of ceramic bodies.[2,3] Electrical conductivity of the ceramic–CNTs composites can also be interesting for heating elements and electrical igniter systems.[4,5] Moreover, the high axial thermal conductivity of CNTs[6] may improve thermal shock resistivity of ceramics.[1] These physical properties suggest that the use of CNTs could lead to the manufacturing of new kinds of multifunctional nano-structured composites.[7]

However, the effectiveness of CNTs on mechanical properties of the ceramic matrix nanocomposites is still matter of debate.[8–20] No tangible improvement or even degradation in the fracture properties and hardness of ceramic–CNT composites was reported by several authors.[8–14] On the other hand numerous investigations demonstrated significant enhancement in hardness, fracture toughness and Young's modulus.[21,22] For instance Zhan et al.[16] reported a notable improvement (from 3.3 to 9.7 MPa $m^{1/2}$) of the indentation fracture toughness in single-wall CNTs reinforced alumina ceramics. Wang et al.,[15] questioned the reliability of Zhen's fracture toughness measurements, while their own analysis using single edge V-notched beam technique on the same composites showed no improvement in toughness.

Tetragonal stabilized zirconia with 3 mol% yttria (YSZ) has been taken into account for many structural applications due to its relatively high strength and fracture toughness (based on – transformation toughening mechanism).[23] In addition, zirconia based ceramics are interesting for several multifunctional applications such as solid oxide fuel cells, oxygen sensors, and ceramic membranes.[24] Incorporation of CNTs and carbon nano-fibers aiming at enhancing mechanical and electrical properties of zirconia has been documented during the last few years. Early investigations on processing and mechani-

* Corresponding author. Tel.: +41 21 693 3389; fax: +41 21 693 4470.
E-mail addresses: mehdi.mazaheri@epfl.ch, mmazaheri@gmail.com (M. Mazaheri).

0955-2219/$ – see front matter © 2010 Elsevier Ltd. All rights reserved.
doi:10.1016/j.jeurceramsoc.2010.11.009

cal/electrical properties of YSZ–CNTs (both single-walled and multi-walled CNTs) were carried out by Sun et al.[13] and Ukai et al.,[8] where addition of 1 wt% (∼2.5 vol.%) CNTs not only did not show any sign of enhancement in parameters such as fracture toughness, fracture strength and hardness compared to monolithic YSZ, but also resulted in the degradation of mechanical properties to some extent. They[8,13] assumed that the low fractional density of the composites on one hand, together with the weak interfacial bonding between the matrix and the CNTs on the other, are the underlying reasons for lower mechanical properties of the composites. A similar tendency in the hot-pressed zirconia/carbon-nanofiber composites, documented by Duszova et al.[10,11] asserted that the aforementioned disappointing mechanical properties could be attributed to a lower density compared to the monolithic YSZ. CNT clustering in the ceramic grain-boundaries, a poor dispersion of fibers into the matrix, and the low volume fractions of CNTs (1.07 wt%) could be other causes for poor toughening. Garmendia et al.[14] used slip casting in order to get a uniform dispersion of CNTs in the zirconia matrix. Although they reported a slight increase in fracture toughness (from 3.8 to 4.0 MPa $m^{1/2}$), the Vickers hardness of CNT–zirconia composites was lower by about 12.5%. While their mixing technique showed a fairly good distribution of CNTs, the lower density of the composite with respect to the monolithic specimen, accompanied by a relatively low fraction of CNTs in the composite (only 1 vol.%), and sintering in a conventional furnace at a high temperature/long time (1350 °C/1 h dwell) may be the critical factors reducing the efficiency of CNT reinforcements. Dusza et al.[9] compared the properties of 3YTZ composites, reinforced with 2 and 3 vol.% carbon-nanofiber, which were processed by two different sintering techniques: spark plasma sintering and hot-pressing. For all compositions, spark plasma sintered (SPS) samples showed a higher fracture toughness and hardness compared to the hot-pressed (HP) ones. Ultra rapid SPS (5 min dwell) technique can preserve the nanotubes from oxidation and transformation to amorphous carbon. High resolution transmission electron microscopy (HR-TEM) micrographs showed a layer of amorphous carbon in the HP sample.[9] Daraktchiev et al.[25] also observed an amorphous layer of carbon in the grain-boundaries of YSZ–CNT composite sintered in a conventional furnace.

The present review of the literature indicates that there are still several difficulties in processing defect free CNT–zirconia composites with improved mechanical properties. In sum, the critical factors needed to develop CNT–ceramic composites with improved mechanical properties can be regarded as follows: (1) homogeneous dispersion of CNTs within the matrix and prohibition of CNTs agglomeration caused by Van der Waals forces; (2) optimum bonding in the interface of CNT–ceramic; i.e. interfacial compatibility and adhesion between CNTs and ceramic matrix as well as strong entangling of the CNTs within the ceramics grains; (3) avoiding damage of the CNTs during processing. The last point has to be carefully taken into account during mixing and high temperature sintering to prevent from nanotube breaking, oxidation and crystal structure destruction. Finally (4) near fully dense composites are required since there is a strong relation between mechanical properties (e.g. hardness) and residual pores after firing. In particular, the presence of nanotubes between the ceramic particles typically delays densification and only in few researches this effect was taken into account so far.

The present study shows a promising method to process fully dense multiwalled carbon nanotube (MWCNT)/3 mol% yttria stabilized zirconia (3YSZ) nanostructured composites by spark plasma sintering (SPS) at a relatively a low temperature and short time, in which MWCNTs are well-dispersed in nanosize-grain zirconia (YSZ). A wide range of nanotube volume fractions (between 0.5 and 5 wt%) was investigated and the reinforcing effect of CNTs has been studied by the measurement of mechanical properties such as the elastic modulus, the hardness and the indentation fracture toughness. Scanning and high-resolution transmission electron microscopy observations have also been performed to support the result interpretation.

2. Experimental procedure

Commercially available, high purity 3 mol% yttria stabilized zirconia (YSZ) powder (Tosoh Co., Japan) and multiwall carbon nanotubes (Arkema, France) were selected as starting powders. Scanning electron microscopy (SEM, XLF-30, Philips, Netherlands) examinations show that the raw YSZ powder is constituted of spherical nanopowders having an average diameter of about 70 nm (Fig. 1a). The CNTs were synthesized by

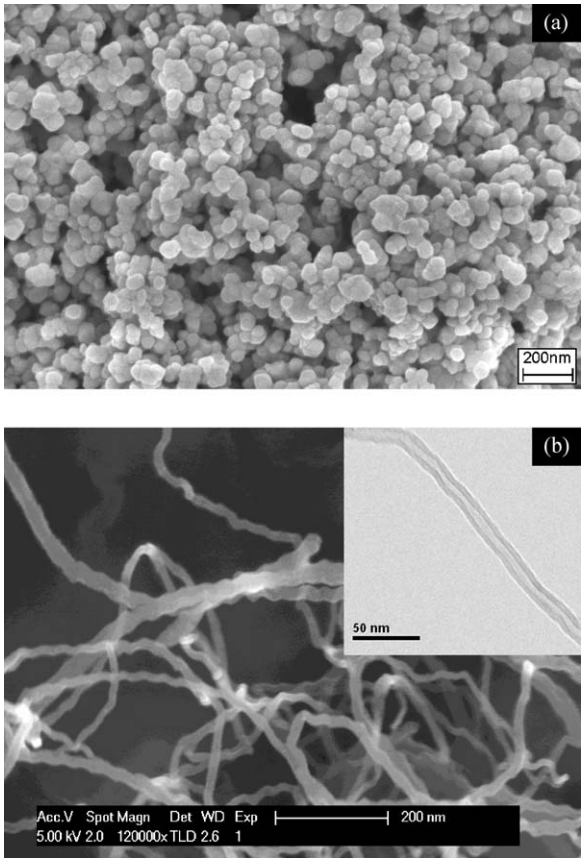

Fig. 1. Electron microscopy micrographs of the as-received powders: (a) yttria stabilized zirconia and (b) pre-dispersed carbon nanotubes.

catalytic chemical vapor deposition. They have a length of about 10–20 μm, a diameter of about 10–20 nm and the number of walls is between 5 and 15 (Fig. 1b). A detailed information on the nanotube synthesis is available in [26].

YSZ powder with 0, 0.5, 1.5, 3 and 5 wt% CNTs, were mixed by attrition milling with zirconia balls for 24 h. The morphology and distribution of the mixtures with variable amount of nanotubes has been analyzed by SEM, and transmission electron microscopy (TEM, CM-20, Philips, Netherlands).

The samples were processed by Spark Plasma Sintering (SPS, FCT GmbH, Germany) under vacuum (10^{-2} mbar). The temperature was measured by means of an optical pyrometer focused on the upper graphite punch, at about 4 mm from the sample. The SPS was carried out with a fixed heating rate of 50 °C min^{-1} under a constant applied pressure of 50 MPa with a soaking time of 2 min. The sintering soak temperature depends on the powder composition and varies between 1250 and 1350 °C. For monolithic zirconia and composites with a low percentage of CNTs (0, 0.5, and 1.5 wt%), 1250 °C was enough to obtain rather dense (relative density >98%) specimens. Instead, for composites with 3 and 5 wt% this temperature had to be increased to 1300 and 1350 °C, respectively. The final sintered specimen size was 40 mm diameter pellets with thickness of about 7 mm.

Throughout all the SPS cycle it was possible to measure the height variation of the powder body (L) precisely and instantaneously. Knowing the instantaneous variation of the sample height, one can calculate the instantaneous relative density (D) based on the following equation (Eq. (1)):

$$D = \left(\frac{L_f}{L}\right) D_f \tag{1}$$

where L_f and D_f are the final sample height and final relative density, respectively.

The densities of sintered samples were determined by Archimedes method in deionized water. The theoretical densities of the composites were calculated according to the rule of the mixtures. The density of graphite (2.25 g cm^{-3}) has been used for CNT. Microstructural observations of sintered composites were carried out on the fracture surface of carbon-coated specimens by high resolution scanning electron microscopy (HR-SEM, FEI-SFEG, Philips, Netherlands). Analytical high-resolution electron microscopy (HR-TEM, CM-300, Philips, Netherlands) was performed with a field emission gun operating at 200 kV on the electron transparent area. HR-TEM specimens were prepared by the tripod polishing method, followed by ion-milling. Raman spectroscopy was used for characterization of the composites. The radiation source was a laser of 514.5 nm wavelength.

Indentation tests were carried out with a diamond Vickers indenter under 20 Kg loads with a dwell of 20 s on carefully polished surfaces. The hardness (HV) was calculated from the diagonal length of the indentation using the following equation

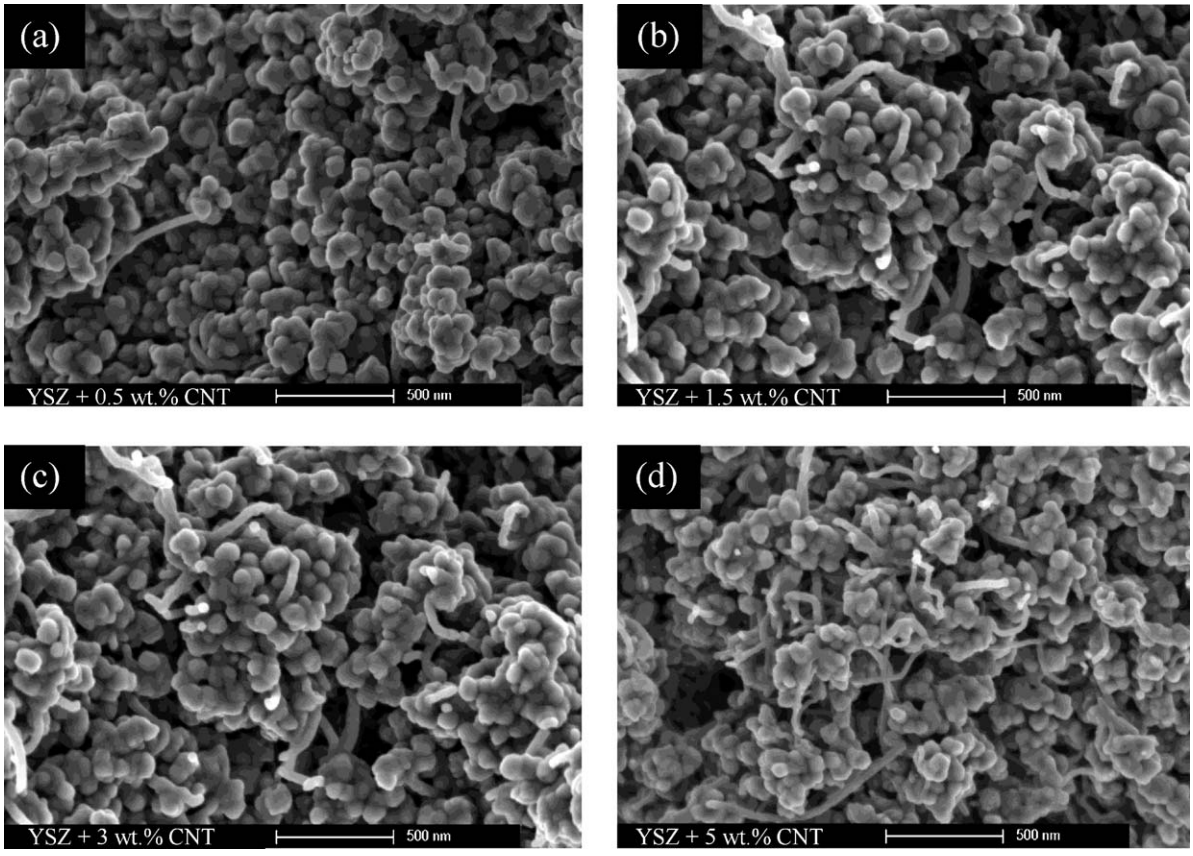

Fig. 2. High resolution scanning electron microscopy of blended yttria stabilized zirconia powder with (a) 0.5 wt%, (b) 1.5 wt%, (c) 3 wt% and (d) 5 wt% carbon nanotubes.

(Eq. (2)):

$$HV = \frac{1.854P}{d^2} \quad (2)$$

where P is the applied load and d is the mean value of the diagonal length. Fracture toughness (K_{Ic}) was determined by measuring the crack length emanating the indentation center indicated by C in the Eq. (3) [27]:

$$K_{Ic} = 0.0016\left(\frac{E}{HV}\right)^{1/2}\left(\frac{P}{C^{3/2}}\right) \quad (3)$$

where E is the Young modulus, HV is the Vickers hardness and P is the load. The crack lengths were measured immediately after indentation using a calibrated optical microscope. At least ten valid measurements were carried out for each sample to calculate the average.

Bar (4 mm × 3 mm × 30 mm) specimens were used for SEVNB fracture toughness measurements using the standard method.[28] The notch preparation was made using a standard procedure. The specimens were bended using 4 point bending fixture with inner and outer span of 10 and 20 mm, respectively.

The Young modulus of monolithic YSZ and of the composites due to the direction of the incident flux was determined by nanoindenter XP with a Berkovitch-type diamond tip, indenting the well-polished surface and monitoring the stiffness to a maximum depth of 1000 nm. At least nine indentations on the surface were performed and averaged.

3. Results

Fig. 2a–d shows the HR-SEM micrographs relative to the mixture of YSZ with various amounts of CNTs after mechanical blending. One can observe well dispersed CNT without traces of CNTs agglomeration within YSZ powder. A TEM image of the 5 wt% CNTs–YSZ powder mixture (Fig. 3) indicates well-mixed and non-damaged CNTs as well.

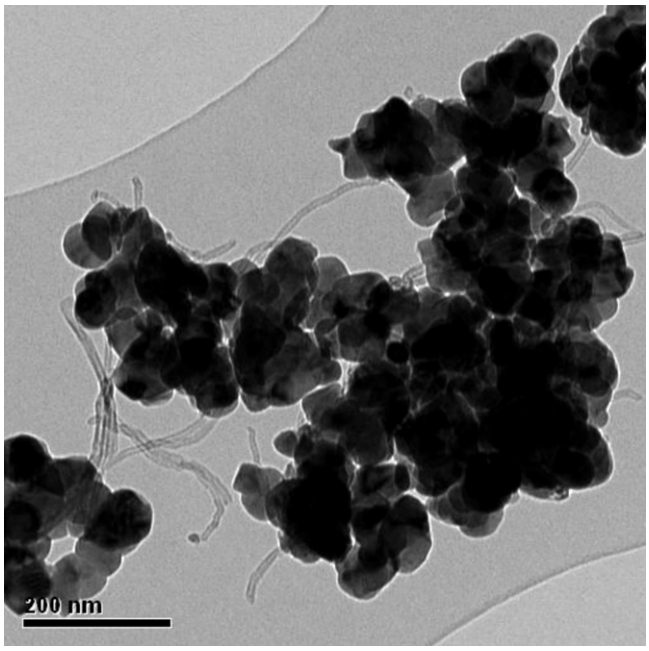

Fig. 3. TEM micrograph of yttria stabilized zirconia–5 wt% CNTs raw composite.

Fig. 4 shows how the composite relative densities vary as a function of temperature with heating (non isothermal sintering) and dwelling at the maximum sintering temperature (isothermal sintering). A typical density–temperature curve pertaining to the majority of materials exhibits a classical sintering sigmoidal shape.[29,30] However, the graphs shift to higher temperatures with

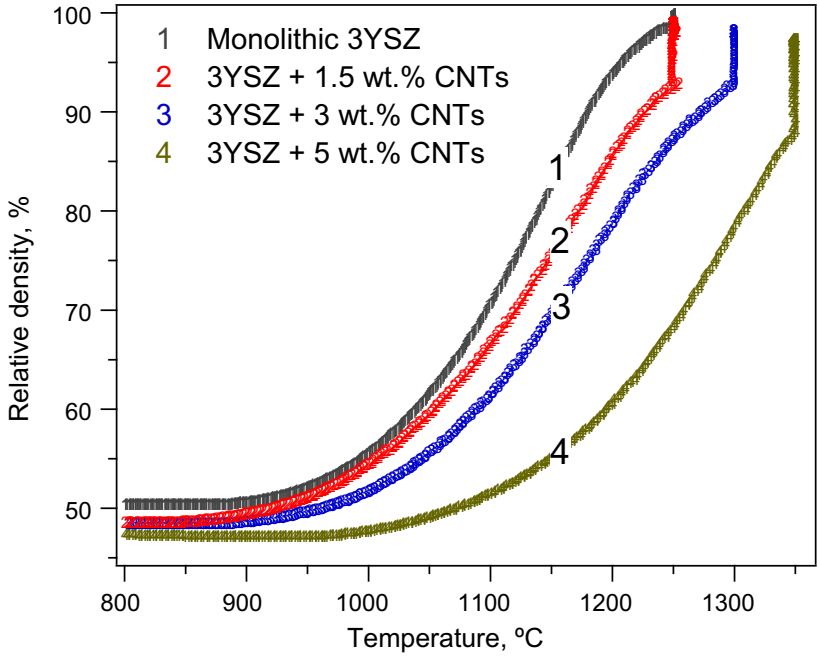

Fig. 4. Densification (relative density vs. temperature) obtained in the monolithic YSZ and composites reinforced with different amounts of CNTs during spark plasma sintering.

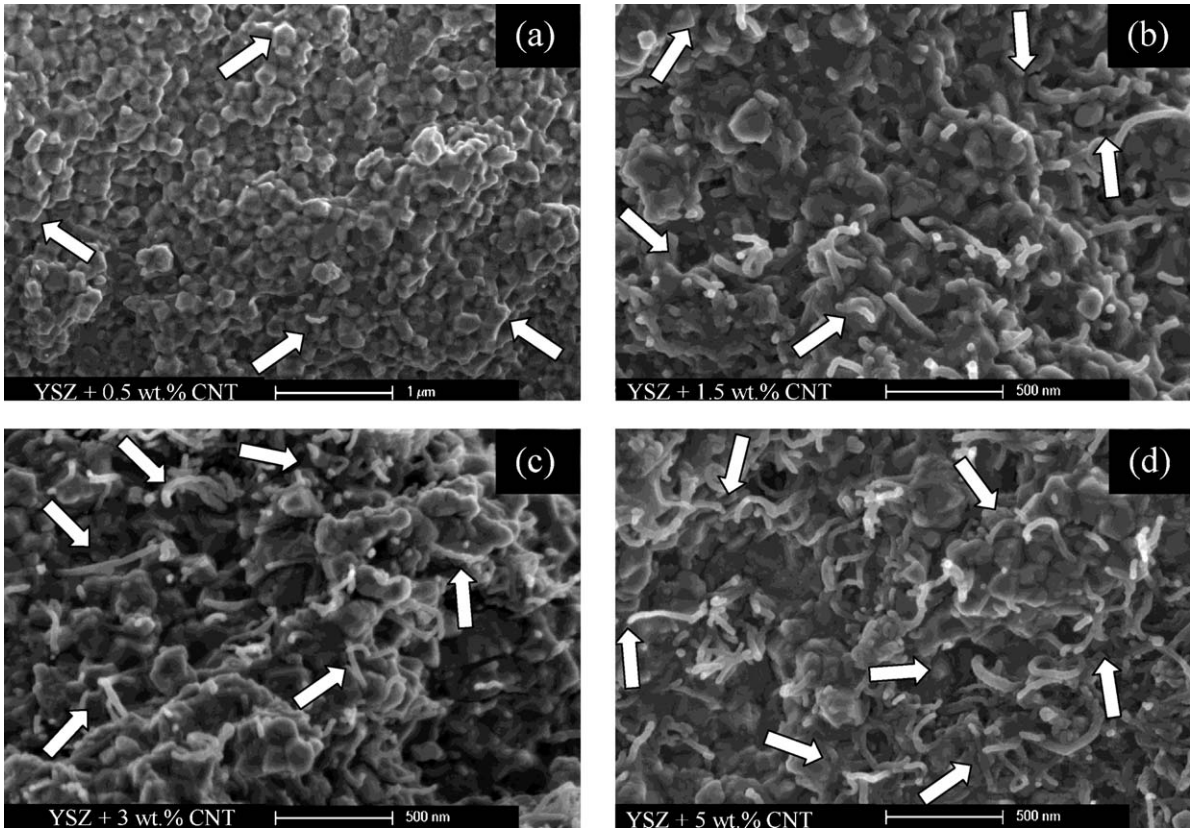

Fig. 5. High resolution SEM of fracture surface of YSZ composites reinforced with (a) 0.5 wt%, (b) 1.5 wt%, (c) 3 wt% and (d) 5 wt% CNTs.

increasing the CNT amount. Three different stages of sintering can be clearly observed in the graphs. In spite of the absence of a significant densification at low temperatures (e.g. less than 900 °C in pure YSZ), the second stage of sintering gave rise to an enhanced densification rate in the second sintering stage (1000–1200 °C). In monolithic YSZ, for instance, one can monitor a dramatic improvement in the values of fractional density from 57% to 95% TD, generated by a temperature increase from 1000 to 1200 °C. In the final stage of sintering, the compaction rate decreases and a further increase in temperature (e.g. from 1200 °C to 1250 °C) results in a slight density enhancement up to 2%. This sintering trend is a common behavior regardless the processed material as also observed by [29,30] for YSZ during spark plasma and conventional sintering. HR-SEM (fracture surface) images of YSZ reinforced with variable amounts of CNTs are represented in Fig. 5a–d. The interesting features can be highlighted as follows: (1) CNTs have surrounded a great fraction of zirconia grains. (2) Most of zirconia grains have maintained a size lower than 100 nm, confirming that CNTs lead to grain refinement. (3) CNTs are homogeneously dispersed in the matrix even at high volume percentages of nanotubes (5 wt% is equal to 12.5 vol.%). (4) The nanotubes have not been damaged both during the powders blending, and upon spark plasma sintering. (5) The fracture mode is mainly intergranular and debonded CNTs from the matrix can be observed on the fracture surfaces (Fig. 5).

Fig. 6 shows the Raman spectra of the as-received CNTs and spark plasma sintered composite reinforced with 5 wt% CNTs. Specific Raman peaks of CNTs,[31] i.e. G and D bands measured in the sintered bodies are nearly identical to those of the raw CNT specimen, providing a definitive evidence for the presence of nanotubes in the YSZ–CNT composites sintered at 1350 °C for 2 min that was the highest sintering temperature compared to other specimens. The slight deviation of both bands to a higher wave number in the sintered composites may be attributed to residual stresses due to the difference between thermal expansion coefficients of CNT and YSZ ceramics.

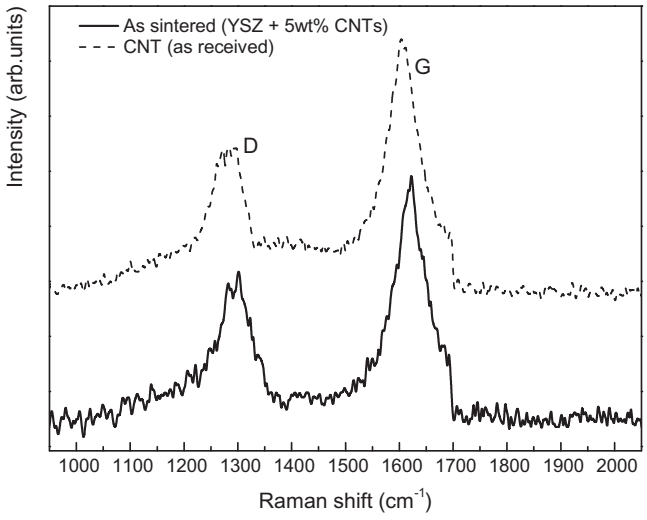

Fig. 6. Raman spectra in the D-band and G-band of as-received CNTs and sintered YSZ composites reinforced with 5 wt% CNTs.

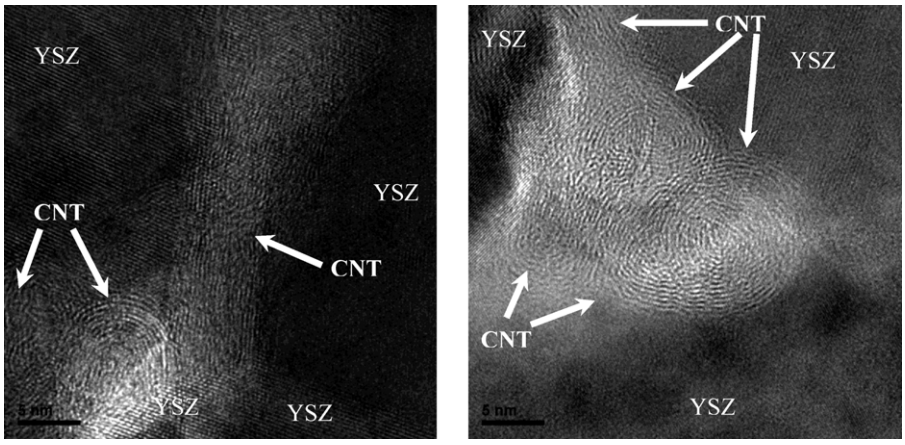

Fig. 7. HR-TEM of sintered YSZ reinforced with 5 wt% CNTs. Randomly oriented non-damaged CNTs in the grain-boundaries are observed.

HR-TEM micrograph of the composites reinforced with 5 wt% CNTs is presented in Fig. 7. Several noticeable features can be pointed out. (1) No trace of amorphous carbon could be detected in the grain boundaries as well as in triple junctions. Similar observations have also been reported for the alumina–CNT system by Vasiliev et al.[32] However, conventionally sintered YSZ/CNT at 1753 K for 3 h,[25] show the presence of an amorphous layer of carbon. (2) Owing to the very fast firing (2 min soaking) and relatively low sintering temperatures in SPS technique, CNTs maintained their structure unchanged during sintering as they were before the process. The fringe spacing in Fig. 7 is 0.34 nm, which is typical of graphite. (3) CNTs in the grain boundaries are randomly oriented (Fig. 7). A cross section of CNT bundles seen from the top as well as a CNT located along the grain boundary can be seen. (4) The interface between CNTs and YSZ grains is flawless and entrapped porosities or defects in the interface could not be detected.

In addition to the sintered fractional density, Table 1 summarizes the mechanical properties, i.e. Vickers hardness, indentation fracture toughness, and the Young modulus of the composites reinforced with various amounts of CNTS, in comparison with monolithic zirconia. All specimens have a fractional density of higher than 98.4% of theoretical density. Therefore, Young's modulus, hardness and toughness should be unaffected by density variations. As a consequence, the significant increase of the Young modulus and of the indentation fracture toughness in the composites should truly be due to the presence of CNTs. For instance, addition of 5 wt% CNTs into monolithic zirconia has ended in a 30% increment in the value of Young's modulus and the indentation fracture toughness improved by a factor of about 2. On the other hand, Vickers hardness does not depend on the CNT content. With regard to fracture toughness measurement, considering the controversial results obtained using the indentation crack length measurements (as explained in introduction),[15] we also used more reliable single edge V-notch bean (SEVNB) technique to measure fracture toughness of monolithic and 5 wt% CNT reinforced composites. The measured K_{Ic} using SEVNB was 6.1 ± 0.15 for monolithic zirconia and 8.1 ± 0.19 for 5 wt% CNT reinforced zirconia composite. Although the increase (32%) in fracture toughness is not as high as what was obtained by the indentation method, it is significant. However, if the indentation fracture toughness does not represent true K_{Ic} the increasing trend with CNT addition is quite clear and remarkable.

4. Discussion

A homogeneous distribution of CNTs on the ceramic grain boundaries (Fig. 6), is essential to improve mechanical properties. However, as previously reported in several studies, CNTs have been found to be highly aggregated into bundles due to Van der Waals attraction.[10,12,13] As it can be observed in TEM micrograph (Fig. 3), the flexibility of CNTs allows them to bend and pass through space between nanopowders and wrap around. This is not possible in YSZ ceramics reinforced with carbon nanofibers.[11] Probably, the flexibility of CNTs can be regarded as one of the major benefits of nanotubes with respect to carbon nanofibers. Moreover, the absence of agglomeration in pre-dispersed/surface-modified CNTs (Fig. 1a) led to a good distribution within the ceramic powder using a conventional mixing technique. Surface modifications create electrical charges on the CNTs surface, acting against agglomeration of the nanotubes.

Table 1
Summary of mechanical properties of YSZ nanocomposites reinforced with different amounts of CNTs.

Sample composition	Relative density (%)	Young's modulus (GPa)	Vickers hardness (GPa)	Indentation fracture toughness (MPa $m^{1/2}$)
YSZ	99.3 ± 0.08	198 ± 15	12.1 ± 0.21	5.8 ± 0.28
YSZ/0.5 wt% CNT	98.9 ± 0.11	206 ± 21	12.2 ± 0.13	6.8 ± 0.33
YSZ/1.5 wt% CNT	98.5 ± 0.13	225 ± 18	12.3 ± 0.11	9.2 ± 0.41
YSZ/3 wt% CNT	98.7 ± 0.09	241 ± 9	12.6 ± 0.21	10.1 ± 0.21
YSZ/5 wt% CNT	98.4 ± 0.06	258 ± 22	12.8 ± 0.18	10.9 ± 0.42

The relative density at low temperatures, before the densification start, can be assumed as the specimens green density, as shown in Fig. 4. It can be seen that the addition of CNTs causes a systematic decrease in the composite green densities under a compressive pressure of 50 MPa. The green relative density of monolithic YSZ was 50.8%, while this value dropped to about 47.4% for the 5 wt% CNT reinforced composite. According to previous investigations[33] the consolidation of ceramic-powders in a rigid die include: (1) sliding and rearrangement of the particles; (2) fragmentation of brittle grains and (3) elastic deformation of bulk compacted powders. At low stress (e.g. lower than 370 MPa for YSZ[34]), sliding and rearrangement of the particles are the dominating mechanisms in nanopowders consolidation. Hence, to explain the lower compaction of zirconia powders in presence of CNTs it can be argued that the ceramic powder sliding and rearrangement have been suppressed. This is in line with TEM observation of raw composite powder (Fig. 3), which shows entangled and kinked nanotubes around the YSZ nanopowder hindering the powders from rearranging freely during compaction.

Based on the densification results (Fig. 4), the addition of CNTs gave rise to a significant increase in the temperatures at which sintering starts (the temperature at which 1% densification occurs) and proceeds. For instance, 1% densification occurred at 936 °C in monolithic YSZ, while the addition of 3 and 5 wt% CNTs hoisted the starting temperature of sintering up to 955 and 1042 °C, respectively. After that densification triggers, the whole sintering procedure develops with temperature. However, the addition of CNTs requires higher temperatures and longer times to complete the densification (Fig. 4). For example, non-isothermal sintering at 1250 °C resulted in a fully dense (98% relative density) monolithic YSZ, while 3 and 5 wt% CNTs reinforced composites have not shown densities higher than 87% and 67%, respectively. The reports, of several authors[9–11,13,14,35] confirm that the addition of CNTs slackens the densification process of YSZ/CNT composites, compared to monolithic zirconia. They all sintered the monolithic YSZ and CNT–YSZ composite at identical sintering conditions (i.e. sintering temperature and dwelling time) and they all obtained a lower density in composites. Duszova et al.[10,11] also showed that final grain size of the sintered composites was smaller than in monolithic zirconia, which evidences that the nanotubes could inhibit the grain growth of zirconia.

Most often, the sintering of traditional whiskers and fiber reinforced composites is limited by differential densification rates. Similar problem may be expected for carbon nanotubes, as well. Recently Bernard-Granger and Guizard[29] have identified the controlling mechanism through the spark plasma sintering of Tosoh-YSZ powder in a wide range of applied pressure and temperature. At intermediate compaction or medium temperature (which is close to the present experiment conditions) they have proposed that densification proceeds with grain-boundary sliding accommodated by the series interface-reaction/lattice diffusion of Zr^{4+} and/or Y^{3+} cations. In a former paper, we have also shown that grain-boundary sliding in YSZ–1.5 wt% CNTs in the temperature range of about 1100–1300 °C could be controlled by the cation lattice diffusion.[36] Therefore, the lower densification rate of CNT reinforced composites with respect to the pure YSZ could be attributed to a slower grain boundary sliding during sintering. In other words, CNTs located in the grain-boundaries could pin them and hinder their movement (sliding or migration) and consequently hinder the densification rate. This hypothesis is supported by recent results that we have obtained by mechanical spectroscopy, which have shown that the mechanical loss of CNT–YSZ composites is lower than in pure YSZ.[36] Such an effect is supposed to be due to the pinning effect of CNTs, which restrict grain-boundary sliding and consequently lowers the mechanical loss due to the relative sliding of grains.

The relatively low density of the CNT–zirconia compacts (compared to the pure zirconia) may be the underlying reason for which recent investigations do not show an improvement of the mechanical properties in CNT reinforced zirconia composites. What should be primarily considered is the strong relationship between microstructural defects such as retained porosities after sintering and mechanical properties, while this issue has been neglected in many papers. Contrary to several investigations in which nanotubes have been damaged by high temperature sintering in a conventional furnace or hot pressing, the present study shows that spark plasma sintering is a promising method to produce full dense materials where the nanotube structure is not altered. Raman spectroscopy results (Fig. 6) in addition to HR-TEM images (Fig. 7) confirm that the processing route chosen here produces a good dispersion of the CNTs in the YSZ matrix without modification of their crystal structure (Fig. 5). The success of this method is mainly due to SPS, which allows lower sintering temperatures, higher heating rates and shorter firing time compared to conventional techniques.

As shown in Table 1 and in Fig. 4, this technique provides almost fully dense composites where CNTs are not damaged and have a strong bonding with the ceramic matrix, which is a prerequisite for enhanced mechanical properties. The underlying mechanisms for toughening, strengthening, and hardening effect of CNTs will be addressed in the following publication.[37]

5. Conclusion

Yttria stabilized zirconia with the addition of carbon nanotubes where sintered by spark plasma sintering (SPS). Dry mixing provided a good dispersion of the CNTs within zirconia particles. The present study shows that SPS is an efficient way for processing composites. Raman spectroscopy and high resolution electron microscopy confirm that the CNTs are not altered by the processing route. The sintering conditions have been optimized to get fully dense materials taking into account that in the presence of CNTs the sintering time and temperature need to be increased. The materials so obtained show a significant improvement of mechanical properties with respect to monolithic zirconia.

Acknowledgements

The authors acknowledge the Swiss National Foundation and the Sixth Framework Program grant no. NMP-2-CT-2006-

026666 for financial support. Hossein Najafi, EPFL-LPMC, is acknowledged for helping with the Nanoindentation measurements.

References

1. Curtin WA, Sheldon BW. CNT-reinforced ceramics and metals. *Materials Today* 2004;**7**(11):44–9.
2. Peigney A. Composite materials: tougher ceramics with nanotubes. *Nature Materials* 2003;**2**(1):15–6.
3. Cho J, Boccaccini AR, Shaffer MSP. Ceramic matrix composites containing carbon nanotubes. *Journal of Materials Science* 2009;**44**(8):1934–51.
4. Rul S, Lefèvre-schlick F, Capria E, Laurent C, Peigney A. Percolation of single-walled carbon nanotubes in ceramic matrix nanocomposites. *Acta Materialia* 2004;**52**(4):1061–7.
5. Shi SL, Liang J. Effect of multiwall carbon nanotubes on electrical and dielectric properties of yttria-stabilized zirconia ceramic. *Journal of the American Ceramic Society* 2006;**89**(11):3533–5.
6. Sivakumar R, Guo S, Nishimura T, Kagawa Y. Thermal conductivity in multi-wall carbon nanotube/silica-based nanocomposites. *Scripta Materilia* 2007;**56**(4):265–8.
7. Padture NP. Multifunctional composites of ceramics and single-walled carbon nanotubes. *Advanced Materials* 2009;**21**(17):1767–70.
8. Ukai T, Sekino T, Hirvonen A, Tanaka N, Kusunose T, Nakayama T, et al. Preparation and electrical properties of carbon nanotubes dispersed zirconia nanocomposites. *Key Engineering Materials*, vol. 317–318; 2006. p. 661–664.
9. Dusza J, Blugan G, Morgiel J, Kuebler J, Inam F, Peijs T, et al. Hot pressed and spark plasma sintered zirconia/carbon nanofiber composites. *Journal of the European Ceramic Society* 2009;**29**(15):3177–84.
10. Duszová A, Dusza J, Tomášek K, Blugan G, Kuebler J. Microstructure and properties of carbon nanotube/zirconia composite. *Journal of European Ceramic Society* 2008;**28**(5):1023–7.
11. Duszova A, Dusza J, Tomasek K, Morgiel J, Blugan G, Kuebler J. Zirconia/carbon nanofiber composite. *Scripta Materialia* 2008;**58**(6):520–3.
12. Zhou JP, Gong QM, Yuan KY, Wu JJ, Chen Yf, Li CS, et al. The effects of multiwalled carbon nanotubes on the hot-pressed 3 mol% yttria stabilized zirconia ceramics. *Materials Science and Engineering A* 2009;**520**(1–2):153–7.
13. Sun J, Gao L, Iwasa M, Nakayama T, Niihara K. Failure investigation of carbon nanotube/3Y-TZP nanocomposites. *Ceramics International* 2005;**31**(8):1131–4.
14. Garmendia N, Santacruz I, Moreno R, Obieta I. Slip casting of nanozirconia/MWCNT composites using a heterocoagulation process. *Journal of the European Ceramic Society* 2009;**29**(10):1939–45.
15. Wang X, Padture NP, Tanaka H. Contact-damage-resistant ceramic/single-wall carbon nanotubes and ceramic/graphite composites. *Nature Materials* 2004;**3**(8):539–44.
16. Zhan GD, Kuntz JD, Wan J, Mukherjee AK. Single-wall carbon nanotubes as attractive toughening agents in alumina-based nanocomposites. *Nature Materials* 2003;**2**(1):38–42.
17. Estili M, Kawasaki A, Sakamoto H, Mekuchi Y, Kuno M, Tsukada T. The homogeneous dispersion of surfactantless, slightly disordered, crystalline, multiwalled carbon nanotubes in α-alumina ceramics for structural reinforcement. *Acta Materialia* 2008;**56**(15):4070–9.
18. Mukhopadhyay A, Chu BTT, Green MLH, Todd RI. Understanding the mechanical reinforcement of uniformly dispersed multiwalled carbon nanotubes in alumino-borosilicate glass ceramic. *Acta Materialia* 2010;**58**(7):2685–97.
19. An L, Xu W, Rajagopalan S, Wang C, Wang H, Fan Y, et al. Carbon-nanotube-reinforced polymer-derived ceramic composites. *Advanced Materials* 2004;**16**(22):2036–40.
20. Estili M, Kawasaki A. Engineering strong intergraphene shear resistance in multi-walled carbon nanotubes and dramatic tensile improvements. *Advanced Materials* 2010;**22**(5):607–11.
21. Peigney A, Garcia FL, Estournès C, Weibel A, Laurent C. Toughening and hardening in double-walled carbon nanotube/nanostructured magnesia composites. *Carbon* 2010;**48**(7):1952–60.
22. Datye A, Wu K-H, Gomes G, Monroy V, Lin H-T, Vleugels J, et al. Synthesis, microstructure and mechanical properties of Yttria Stabilized Zirconia (3YTZP)–Multi-Walled Nanotube (MWNTs) nanocomposite by direct in-situ growth of MWNTs on zirconia particles. *Composites Science and Technology* 2010;**70**(14):2086–92.
23. Garvie RC, Hannink RHJ, Pascoe RT. Ceramic steel? *Nature* 1975;**258**:703–4.
24. Minh NQ. Ceramic fuel cells. *Journal of the American Ceramic Society* 1993;**76**(3):563–88.
25. Daraktchiev M, Van De Moorto B, Schaller R, Couteau E, Forro L. Effects of carbon nanotubes on grain boundary sliding in zirconia polycrystals. *Advanced Materials* 2005;**17**(1):88–91.
26. http://www.graphistrength.com.
27. Anstis GR, Chantikul P, Lawn BR, Marshall DB. A critical evaluation of indentation techniques for measuring fracture toughness: I. Direct crack measurements. *Journal of the American Ceramics Society* 1981;**64**(9):533–8.
28. Kubler J. Fracture toughness of ceramics using the SEVNB method: from a preliminary study to a standard test method. In: Salem JA, Quinn GD, Jenkins MG, editors. *Fracture resistance testing of monolithic and composite brittle*. West Conshohocken, PA: American Society for Testing and Materials; 2002. p. 93–106.
29. Bernard-Granger G, Guizard C. Spark plasma sintering of a commercially available granulated zirconia powder: I. Sintering path and hypotheses about the mechanism(s) controlling densification. *Acta Materialia* 2007;**55**(10):3493–504.
30. Mazaheri M, Simchi A, Dourandish M, Golestani-Fard F. Master sintering curves of a nanoscale 3Y-TZP powder compacts. *Ceramics International* 2009;**35**(2):547–54.
31. Delhaes P, Couzi M, Trinquecoste M, Dentzer J, Hamidou H, Vix-Guterl C. A comparison between Raman spectroscopy and surface characterizations of multiwall carbon nanotubes. *Carbon* 2006;**44**(14):3005–13.
32. Vasiliev AL, Poyato R, Padture NP. Single-wall carbon nanotubes at ceramic grain boundaries. *Scripta Materialia* 2007;**56**(6):461–3.
33. Carry PBaC. From powders to sintered pieces: forming, transformations and sintering of nanostructured ceramic oxides. *Powder Technology* 2002;**128**(2–3):248–55.
34. Mazaheri M, Valefi M, Hesabi ZR, Sadrnezhaad SK. Two-step sintering of nanocrystalline $8Y_2O_3$ stabilized ZrO_2 synthesized by glycine nitrate process. *Ceramics International* 2009;**35**(1):13–20.
35. Ionascu C. High temperature mechanical spectroscopy of fine-grained zirconia and alumina containing nano-sized reinforcements. Thesis No. 3994. Lausanne: EPFL; 2008.
36. Mazaheri M, Mari D, Schaller R. High temperature mechanical spectroscopy of yttria stabilized zirconia reinforced with carbon nanotubes. *Physica Status Solidi A* 2010;**207**(11):2456–60.
37. Mazaheri M, Mari D, Hesabi ZR, Schaller R, Fantozzi G. Multi-walled carbon nanotube/nanostructured zirconia composites: outstanding mechanical properties in a wide range of temperature; submitted for publication.